Communications

Duffy Method for Evaluation of Weakly Singular SIE Potential Integrals Over Curved Quadrilaterals With Higher Order Basis Functions

Ana B. Manić, Miroslav Djordjević, and Branislav M. Notaroš

***Abstract*—A Duffy method for singularity cancellation is proposed for evaluation of weakly singular potential integrals defined on generalized curved parametric quadrilateral patches with polynomial basis functions. Such integrals arise in evaluation of Galerkin matrix elements in method-of-moments analysis of antennas and scatterers in cases of coincident source and test elements. Examples demonstrate that the proposed Duffy method is more accurate, more rapidly converging with the increase of orders of Gauss-Legendre integration formulas, and faster to execute than four other methods for singularity treatment considered in the study.**

***Index Terms*—Coordinate transformation, curved parametric elements, Duffy method, higher order modeling, singular potential integrals, singularity cancellation, singularity extraction.**

I. Introduction

In analysis of antennas and scatterers based on the method of moments (MoM) in conjunction with the surface integral equation (SIE) approach [1], one of the most important problems in the development of a MoM-SIE technique is the treatment of weakly singular potential two-dimensional (2-D) integrals. Such integrals are involved in the self-terms of the Galerkin impedance matrix, with the testing patch coinciding with the source patch, namely, when an observation (testing) point belongs to the source patch (with basis functions). This problem is even more pronounced and challenging when higher order basis functions are used for the approximation of surface currents, and especially when such functions are defined on curved surface (boundary) elements (patches) employed for geometrical modeling of the structure [2].

Singularity extraction (subtraction) methods for singular integrals consist of analytical integration of a principal singular part of the integrand and numerical integration of the residual using quadrature formulas [1]–[3]. Singularity cancellation methods are based on coordinate transformations, i.e., on mapping of the integration domain to a new parametric domain such that the Jacobian of the transformation cancels out the singular term in the integrand. A typical representative of this approach is the Duffy method [4], originally proposed for a volumetric integration domain [5].

However, most of the previous research in this area has been devoted to handling the singularities on planar triangular patches with low-order current approximations, typically in the form of Rao-Wilton-Glisson (RWG) basis functions, e.g., [3], [6]–[11]. Overall, there seems to be a lack of reported results on the treatment of singular potential integrals involved in the self Galerkin MoM-SIE impedance matrix entries for curved surface elements with higher order basis functions, the only methods for singularity extraction or cancellation in such cases being those presented in [1], [2], [12]–[16]. In particular, a singularity extraction method for curved quadrilateral elements with higher order hierarchical polynomial vector basis functions is implemented in [1], [2]. A polar transformation method for singular potential integrals over curved quadrilateral elements with higher order hierarchical polynomial bases is proposed in [12]. Rectangular transformation methods for singularity cancellation are applied to solve potential integrals over curved quadrilateral elements with higher order hierarchical polynomial bases in [13] and [14]. The Duffy method is applied to evaluation of singular integrals over curvilinear triangles in [15], [16]. There is also a lack of evaluations and assessments of the accuracy and convergence properties of various possible singularity treatment and integration methods, for different locations of singular points in parametric domains, different basis functions on flat or curved surface elements, and overall.

This communication presents a Duffy method for singularity cancellation to evaluate singular potential integrals involved in the self Galerkin MoM-SIE impedances defined on Lagrange-type generalized curved parametric quadrilateral surface elements of arbitrary geometrical orders with polynomial basis functions of arbitrary current-approximation orders. The communication also presents a comparison of the integration accuracy when using five different methods for evaluation of singular potential integrals, implemented in the same code. The methods are: (i) the singularity extraction method [2], (ii) the Duffy method for singularity cancellation (proposed in this communication), (iii) the polar transformation method for singularity cancellation [12], (iv) the quadratic rectangular transformation method for singularity cancellation [13], and (v) the cubic rectangular transformation method [14]. We show that overall, of the five integration methods considered, the proposed Duffy method for singularity cancellation comes out to be the most accurate, the most rapidly converging with the increase of the order of integration formulas, and the fastest to execute.

II. Theory

We consider a MoM-SIE model of an antenna or scatterer built using generalized curved parametric quadrilaterals of arbitrary geometrical ordersK_u and $K_v (K_u, K_v \geq 1)$, shown in Fig. 1 and analytically described in the parametric $u-v$ domain as [1]

$$\mathbf{r}(u,v) = \sum_{i=0}^{K_u} \sum_{j=0}^{K_v} \mathbf{r}_{ij} u^i v^j, \quad -1 \leq u, v \leq 1 \tag{1}$$

where $\mathbf{r}_{ij}$ are constant vector coefficients related to position vectors of interpolation nodes defining the quadrilateral. When these elements are used in conjunction with higher order polynomial basis functions, all entries of the Galerkin impedance matrix can be found as linear combinations of 2-D/2-D Galerkin integrals [1], which, for the case of testing

Manuscript received May 28, 2012; revised December 29, 2013; accepted February 16, 2014. Date of publication March 05, 2014; date of current version May 29, 2014. This work was supported by the National Science Foundation under grant ECCS-1002385 and by the Serbian Ministry of Education and Science under grant TR-36002.

A. B. Manić and B. M. Notaroš are with Colorado State University, Department of Electrical and Computer Engineering, Fort Collins, CO 80523-1373 USA (e-mail: anamanic@engr.colostate.edu; notaros@colostate.edu).

M. Djordjević is with ICT College, 11000 Belgrade, Serbia (e-mail: miroslav@ieee.org).

Color versions of one or more of the figures in this communication are available online at http://ieeexplore.ieee.org.

Digital Object Identifier 10.1109/TAP.2014.2309971

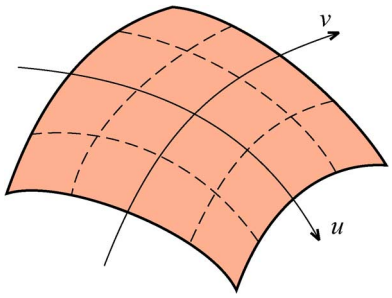

Fig. 1. Generalized curved parametric quadrilateral defined by (1).

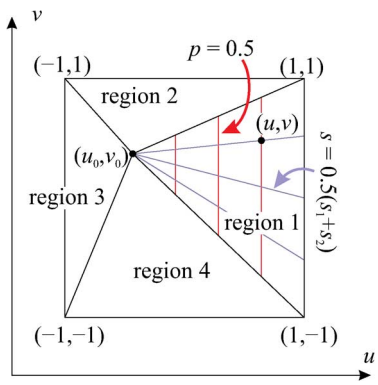

Fig. 2. Duffy method for singularity cancellation: subdivision of the parametric $u-v$ square domain into four parametric triangles with local constant p and constant s parametric lines in triangular region 1.

and basis functions being defined on the same patch (self Galerkin integrals), contain the following singular inner 2-D basic potential integrals computed at an observation (testing) point (u_0, v_0) belonging to the source quadrilateral patch:

$$I_{mn} = \int_{-1}^{1}\int_{-1}^{1} u^m v^n g(R)\mathrm{d}u\mathrm{d}v, \quad g(R) = \frac{\mathrm{e}^{-\mathrm{j}kR}}{4\pi R}$$
$$k = 2\pi f\sqrt{\varepsilon_0\mu_0}, \quad R = |\mathbf{r}(u,v) - \mathbf{r}(u_0,v_0)| \tag{2}$$

with g being the free-space Green's function, f the operating frequency of the antenna/scatterer, and R the distance of the source point (u, v) from the point (u_0, v_0), referred to as the singular point. When the two points coincide, R is zero, and a special treatment of the singularity is needed.

A. Duffy Method for Singularity Cancellation

We propose a Duffy method to solve integrals in (2), which is based on subdividing the parametric $u-v$ square domain into four parametric triangles defined by the singular point and the vertices of the square, as shown in Fig. 2 (also see [10] and [17]). Note that this is a modification in the spirit of the original Duffy method initially proposed for a 3-D domain of integration [5], which would imply a subdivision of the parametric square into eight right-angled triangles (much like in Fig. 4). Each triangle in Fig. 2, having the singular point as one of its vertices, is then independently mapped into a new $p-s$ domain as illustrated in Fig. 2, for one of the regions. Note also that the Duffy method in [15] is implemented for triangle local coordinates, while in [16] it is further developed using mapping of a curvilinear triangle to an isosceles right triangle.

TABLE I
PARAMETERS OF THE DUFFY MAPPING IN (3) FOR THE FOUR TRIANGULAR REGIONS IN FIG. 2

Region 1	Region 2	Region 3	Region 4
$u=a, v=b$	$v=a, u=b$	$u=a, v=b$	$v=a, u=b$
$s_1^1 = -1-v_0$	$s_1^2 = -1-u_0$	$s_1^3 = -1-v_0$	$s_1^4 = -1-u_0$
$s_2^1 = 1-v_0$	$s_2^2 = 1-u_0$	$s_2^3 = 1-v_0$	$s_2^4 = 1-u_0$
$c = 1-u_0$	$c = 1-v_0$	$c = -1-u_0$	$c = -1-v_0$

Mapping to the $p-s$ domain differs for different triangles in Fig. 2 but can be expressed in a unified way as follows:

$$a = a_0 + pc,\ b = b_0 + ps,\ 0 \le p \le 1,\ s_1 \le s \le s_2,\ c = \text{const} \tag{3}$$

with coordinates a and b standing for either u or v such that a is always constant on the triangle edge across the singular vertex, while b is the other parametric coordinate. With this notation, Table I provides mapping parameters for each region (triangle). Based on (3), the Jacobian of the mapping can be defined and computed, for every triangle, as

$$\Im = \begin{vmatrix} \frac{\partial a}{\partial p} & \frac{\partial b}{\partial p} \\ \frac{\partial a}{\partial s} & \frac{\partial b}{\partial s} \end{vmatrix} = p|c|. \tag{4}$$

Combining (3) and (1), the radial distance from the singular point in triangular region l in Fig. 2 can be expressed as a polynomial in p with coefficients $\mathbf{d}$ being functions of s, as follows [note that the only term in the binomial expansion of $u^i v^j$ using (3) that does not contain p is $u_0^i v_0^j$]:

$$R^l = \left|\sum_{i=0}^{K_u}\sum_{j=0}^{K_v} \mathbf{r}_{ij}\left(u^i v^j - u_0^i v_0^j\right)\right|$$
$$= p\left|\mathbf{d}_1^l + \sum_{i=2}^{K_u+K_v} \mathbf{d}_i^l p^{i-1}\right|, \quad l = 1,2,3,4. \tag{5}$$

Hence, the singular integral over region l can be expressed using (2), (5), and (4) in a way that removes (cancels) the singularity,

$$I_{mn}^l = \frac{1}{4\pi}\int_0^1\int_{s_1^l}^{s_2^l} \frac{u^m v^n}{R^l}\mathrm{e}^{-\mathrm{j}kR^l}\Im\mathrm{d}p\mathrm{d}s$$
$$= \frac{|c|}{4\pi}\int_0^1\int_{s_1^l}^{s_2^l} \frac{u^m v^n \mathrm{e}^{-\mathrm{j}kR^l}\mathrm{d}p\mathrm{d}s}{\left|\mathbf{d}_1^l + \sum_{i=2}^{K_u+K_v}\mathbf{d}_i^l p^{i-1}\right|} \tag{6}$$

namely, the singular dependence on the p coordinate in (5) is canceled by p in the expression for the Jacobian in (4), so the integral in the final form in (6) can be evaluated in a straightforward fashion numerically, using quadrature (e.g., Gauss-Legendre) formulas. Finally, the contributions of individual triangles are added up for the total potential integral, $I_{mn} = I_{mn}^1 + I_{mn}^2 + I_{mn}^3 + I_{mn}^4$.

B. Four Other Integration Methods Used for Comparison

Singularity Extraction Method: The method of extracting the singularity consists of analytical integration of a principal singular part of the

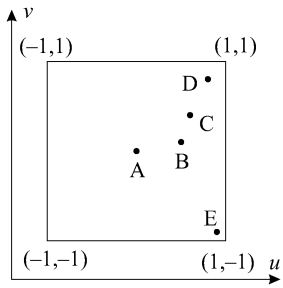

Fig. 3. Five different choices of the singular point (u_0, v_0), with parametric coordinates given in Table II, in the $u-v$ parametric domain, over curved quadrilaterals in Fig. 1.

integrand over a (generally not rectangular) parallelogram whose surface is tangential to the surface of the generalized quadrilateral at the singular point, and numerical integration of the rest using Gauss-Legendre quadrature formulas [1], [2]. The parallelogram is defined by the unitary vectors of the generalized quadrilateral at the singular point [1]. The singular integral is evaluated analytically as in [3], while the remainder is well behaved in the vicinity of the point (u_0, v_0) and can be accurately integrated numerically.

Polar Transformation Method for Singularity Cancellation: Polar transformation [12] uses the same triangulation as in the Duffy method in Fig. 2 while mapping the parametric $u-v$ domain into a new $\rho-\theta$ domain, with a standard meaning of the radial coordinate, ρ, and angular coordinate, θ, in the polar coordinate system centered at the singular point, (u_0, v_0), in the $u-v$ domain.

Quadratic and Cubic Rectangular Transformation Methods for Singularity Cancellation: Rectangular transformation methods [13], [14], [18] subdivide the parametric $u-v$ square domain into four rectangular regions whose common vertex is the singular point. The rectangular transformation for SIE integrals is applied with mapping order $t=2$ (quadratic transformation) in [13], while [14] implements the same transformation with mapping order $t=3$ (cubic transformation).

III. Numerical Results and Discussion

We compare the integration accuracy when using five different methods for evaluation of singular potential integrals, described in the previous section. In the first set of examples, the integrals are computed for five different locations of the singular point defined in the $u-v$ parametric domain as shown in Fig. 3 and specified in Table II. The choice of singular points is made so that it reflects evaluation of singular integrals needed for the assembly of self Galerkin impedance matrix entries. However, the same integration schemes can be applied when singular points belong to an edge or coincide with a vertex of the source domain; in such cases, one would just have a different number of regions after the subdivision of the integration domain. All results are given in terms of the relative integration error computed as

$$\delta = \frac{|I_{mn} - \tilde{I}_{mn}|}{|\tilde{I}_{mn}|} \tag{7}$$

where $\tilde{I}_{mn}$ is the reference "exact" value of the integral. All computations are performed in double machine precision.

A. Integral With Constant Basis Functions Over a Square Plate

As the first example, we consider the integral in (2) for $m=n=0$, namely, with constant basis functions, over a square flat plate of side length $a=2$ m, at a frequency $f=300$ MHz, so that $a=2\lambda$, with λ standing for the free-space wavelength. With reference to Fig. 4, the

TABLE II
Parametric Coordinates of Singular Points in Fig. 3

Point A	Point B	Point C	Point D	Point E
$u_0=0$	$u_0=0.5$	$u_0=0.6$	$u_0=0.8$	$u_0=0.9$
$v_0=0$	$v_0=0.1$	$v_0=0.4$	$v_0=0.8$	$v_0=-0.9$

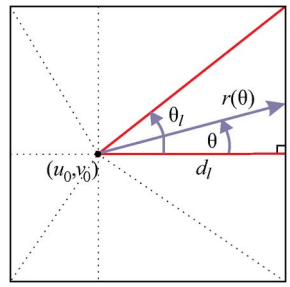

Fig. 4. For integration in (8) over one of the eight right-angled triangles constituting a square flat plate, to compute the reference "exact" value of the integral I_{00}.

TABLE III
Reference Values of Integral $\tilde{I}_{00}$ Over a $2\lambda \times 2\lambda$ Flat Plate for Singular Points in Fig. 3

Point A	0.0390728194148081 - 0.0338074127356726j
Point B	- 0.0104077559218362 - 0.0873743257011760j
Point C	- 0.019482990210943 - 0.117888060820110j
Point D	0.0370913362751421 - 0.0717465899269053j
Point E	0.0379659704128063 - 0.0400119796261574j

"exact" value $\tilde{I}_{00}$ in this special case (flat plate) can be obtained by first analytically transforming the 2-D integral in u and v as

$$\begin{aligned}\tilde{I}_{00} &= \int_{-1}^{1}\int_{-1}^{1} \frac{\mathrm{e}^{-\mathrm{j}kR}\mathrm{d}x\mathrm{d}y}{4\pi R} \\ &= \sum_{l=1}^{8}\int_{0}^{\theta_l}\int_{0}^{r(\theta)} \frac{\mathrm{e}^{-\mathrm{j}k\rho}\mathrm{d}\rho\mathrm{d}\theta}{4\pi} \\ &= \sum_{l=1}^{8}\int_{0}^{\theta_l} \frac{1-\mathrm{e}^{\frac{-\mathrm{j}kd_l}{\cos\theta}}}{\mathrm{j}k4\pi}\mathrm{d}\theta \end{aligned} \tag{8}$$

and then numerically solving the final non-singular 1-D integrals in θ. $\tilde{I}_{00}$ integral values are given in Table III. Fig. 5 shows the error in (7) against the orders of Gauss-Legendre integration formulas, i.e., numbers of integration points, in each of the region's local directions, NGL (the same in both directions), for five different singular points in Fig. 3 and five different integration methods.

Based on Fig. 5(a)–(c), we conclude that, for singular points A, B, and C, the Duffy method and the polar transformation method for singularity cancellation perform the best, with the Duffy method converging even faster in some cases than the latter method. We also observe that accuracy and convergence properties of the singularity extraction method noticeably outperform the cubic rectangular transformation method, and especially the quadratic rectangular transformation method. From Fig. 5(d)–(f), we realize that the Duffy method is considerably more accurate and faster converging than the polar transformation method for some specific choices of singular points, i.e., points D and E, and that the singularity extraction method features the highest convergence rate of all the methods for smaller values of NGL.

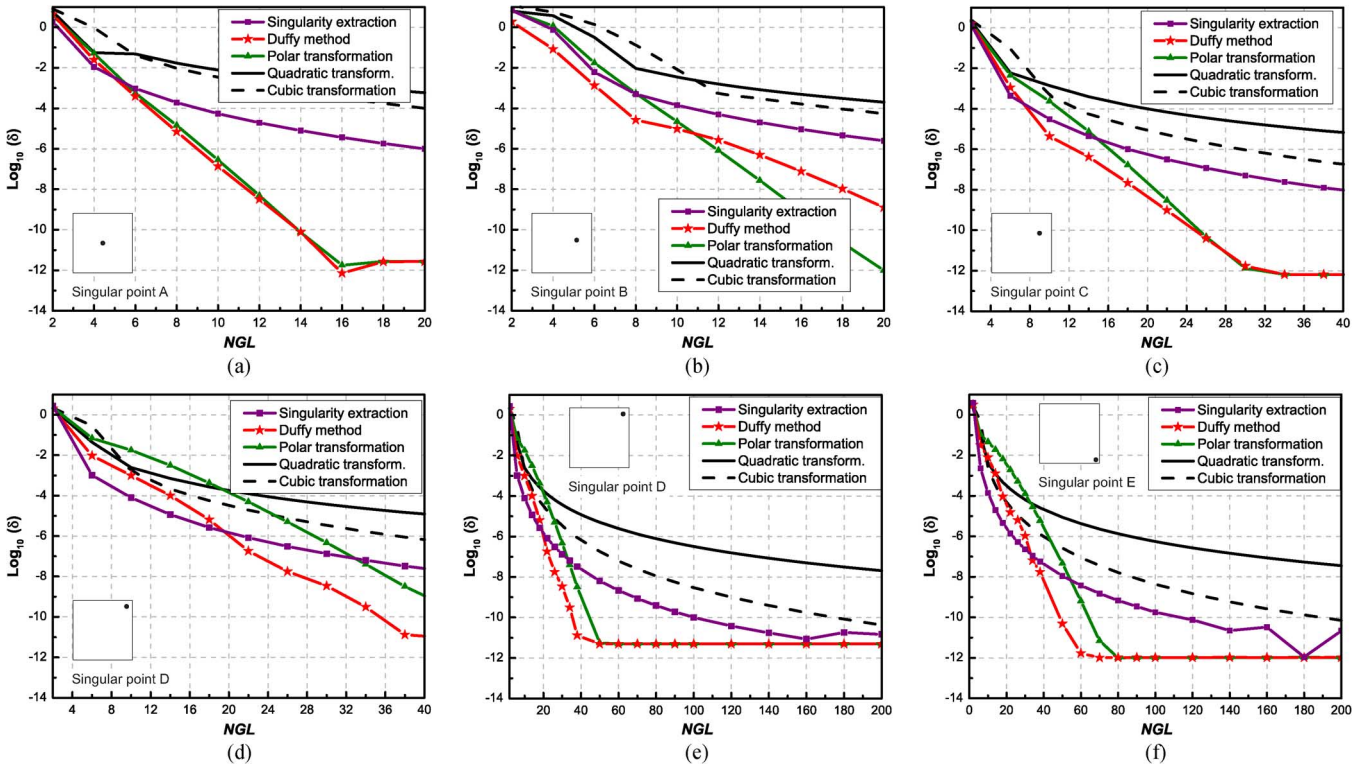

Fig. 5. Evaluation of the integral I_{00} (for $m = n = 0$) in (2) over a square flat plate using the singularity extraction method, the Duffy method for singularity cancellation, the polar transformation method for singularity cancellation, the quadratic rectangular transformation method for singularity cancellation, and the cubic rectangular transformation method: integration error in (7) against the order of Gauss-Legendre integration formulas, NGL, for five different singular points in Fig. 3 [$\tilde{I}_{00}$ is computed as given in (8) and Fig. 4].

Note, however, that this is electrically a rather large patch, namely, the $2\lambda \times 2\lambda$ plate considered as a single MoM element. Smaller patches, e.g., those on the order of $\lambda \times \lambda$ and $0.5\lambda \times 0.5\lambda$, also used in higher order MoM-SIE techniques, and especially electrically small patches measuring $0.1\lambda \times 0.1\lambda$ and less, characteristic for low-order MoM-SIE techniques, require far lower values of NGL for a given accuracy of integration and a given machine precision (double precision).

Overall, when NGL is not limited, as shown in Fig. 5(e)–(f), the best convergence behavior is achieved by the Duffy method. While for some singular points and lower values of NGL, the singularity extraction method reaches certain accuracy levels the fastest, further improvement of its accuracy at the expense of adopting higher NGL values is rather slow. On the other hand, both the Duffy method and the polar transformation method exhibit a logarithmic-type of convergence with increasing NGL.

Among the results for all singular points, the worst accuracies and convergence behaviors for all integration methods are those in Fig. 5(f). The singular point E in Fig. 3 thus comes out to be the worst-case scenario for the evaluation of the integral I_{00} using any of the methods, and the error graphs in Fig. 5(e) and (f) may be considered as defining and limiting the accuracy and convergence properties of the individual methods as long as the integration performance at specific singular points is concerned.

Table IV provides information on computation times for the five integration methods, for singular point A and $NGL = 20$. We see that, out of all the methods, the Duffy method, being the simplest, is the fastest to execute.

TABLE IV
COMPUTATION TIMES FOR FIVE INTEGRATION METHODS (INTEGRAL I_{00} OVER A SQUARE FLAT PLATE, SINGULAR POINT A, AND $NGL = 20$)

Singularity extraction	Duffy method	Polar transform.	Quadratic transform.	Cubic transform.
390 μs	328 μs	359 μs	390 μs	374 μs

B. Integral With High-Order Basis Functions Over a Spherical Patch

In the second example, we evaluate the integral in (2) for a selection of high-order basis functions given by $m = 2$ and $n = 6$ over a curved quadrilateral patch (in Fig. 1) of the fourth geometrical order, namely, with $K_u = K_v = 4$ in (1), modeling one-sixth of a sphere of radius $a = 1.2732$ m, at a frequency $f = 300$ MHz, with the patch being about 2λ across. Shown in Fig. 6 is the geometry of the patch and the error in (7) against the order of Gauss-Legendre integration formulas, NGL, for singular points A, B, C, D, and E in Fig. 3 and the five different integration methods. Based on the results in the previous example, as well as on extensive numerical investigations of the five methods in this (second) example, it is established that both the Duffy method and the polar transformation method for singularity cancellation with the order of Gauss-Legendre integration formulas adopted to be as high as $NGL = 200$ can reliably be considered as the fully converged and highly accurate, with negligible differences between results of the two methods. For all five singular points analyzed, the relative difference between results obtained using Duffy and polar transformation methods with $NGL = 200$ is less than 1.5×10^{-14}. Therefore, in this example, we choose the solution by the Duffy method with $NGL = 200$ as the reference ("exact") result for $\tilde{I}_{26}$ in (7), with the reference values given in Table V.

Conclusions about the accuracy and convergence properties of different integration methods, and their relative advantages and shortcomings, for specific singular points and overall, are similar to those drawn in the previous example. In addition, we realize that all the methods perform well in Fig. 6(a) since the singular point location A

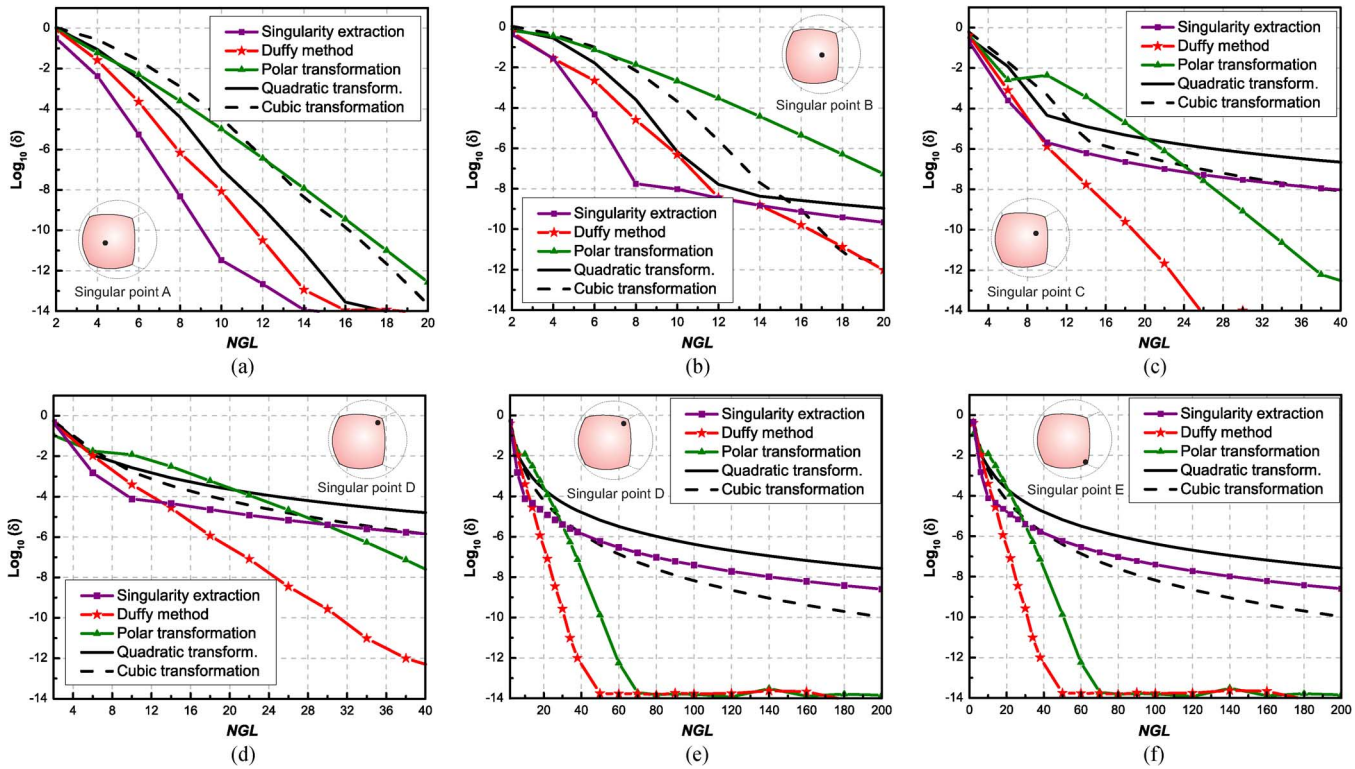

Fig. 6. Evaluation of the integral I_{26} (for $m = 2$ and $n = 6$) in (2) over a spherical patch using five different integration methods: integration error in (7) against the order of integration formulas, NGL, for five different singular points ($\tilde{I}_{26}$ is computed by the Duffy method with $NGL = 200$).

TABLE V
REFERENCE VALUES OF INTEGRAL $\tilde{I}_{26}$ OVER A $2\lambda \times 2\lambda$ CURVED PATCH MODELING ONE-SIXTH OF A SPHERE FOR SINGULAR POINTS GIVEN IN FIG. 3

Point A	0.0124967595839862 - 0.0012958743848867 5j
Point B	-0.000465975239161153 + 0.00318092837694706j
Point C	-0.00558811841514885 - 0.00543831056714150j
Point D	0.0176400704430661 - 0.0199165023639411j
Point E	0.0281932219071943 - 0.0194326435061862j

yields a non-singular integral (2), due to the polynomial part of the integrand having higher-order zeros. Fig. 6(b)–(f) demonstrate that the polar transformation method offers substantially slower convergence for singular integrals defined over curved patch when compared to ones defined on the flat geometry. Furthermore, for low orders of integration formulas, five methods result in a comparable precision; however, with the increase in number of integration points, Duffy and polar transformation methods yield a convergence superior to other methods.

C. Computation of a Full 2-D/2-D Self Galerkin Integral Over a Half of an Oblate Spheroid

As the final example, we evaluate a full 2-D/2-D self Galerkin integral (used in assembly of Galerkin impedance matrix entries)

$$I_{m_\mathrm{t} n_\mathrm{t} m_\mathrm{b} n_\mathrm{b}} = \int_{-1}^{1}\int_{-1}^{1} u_\mathrm{t}^{m_\mathrm{t}} v_\mathrm{t}^{n_\mathrm{t}} \left(\int_{-1}^{1}\int_{-1}^{1} u_\mathrm{b}^{m_\mathrm{b}} v_\mathrm{b}^{n_\mathrm{b}} g(R)\mathrm{d}u_\mathrm{b}\mathrm{d}v_\mathrm{b} \right) \mathrm{d}u_\mathrm{t}\mathrm{d}v_\mathrm{t} \quad (9)$$

defined on a curved quadrilateral patch with $K_u = K_v = 4$ modeling a half of an oblate spheroid with the maximum dimension of 2λ. The orders of testing and basis polynomial functions are set to $m_\mathrm{t} = n_\mathrm{t} = 4$ and $m_\mathrm{b} = n_\mathrm{b} = 6$, respectively. Based on conclusions in [19], we adopt $NGL = 6$ for the regular Gauss-Legendre scheme used for the calculation of the outer, well-behaved, 2-D integral, while NGL for the inner 2-D integration is ranged as depicted in Fig. 7. The patch geometry and convergence results for the integral I_{4466} are shown in Fig. 7, with the same observations and conclusions in terms of the performance of different integration methods as in the previous examples.

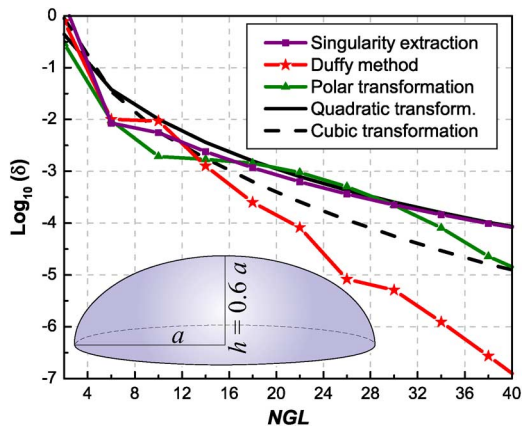

Fig. 7. Evaluation of the 2-D/2-D self Galerkin integral I_{4466} over a large curved quadrilateral patch with $K_u = K_v = 4$ modeling a half of an oblate spheroid.

IV. CONCLUSIONS

This communication has proposed a Duffy method for singularity cancellation to evaluate weakly singular potential integrals involved in the self Galerkin impedances in MoM-SIE analysis of antennas and scatterers. The impedances are defined on Lagrange-type generalized

curved parametric quadrilateral surface elements of arbitrary geometrical orders with polynomial basis functions of arbitrary current-approximation orders. In addition, the communication is considered as a step forward in overcoming the current lack of evaluations of various possible singularity treatment and integration methods, and assessments of the accuracy and convergence properties of different methods, and their relative advantages and shortcomings, for different locations of singular points in parametric domains, different basis functions on flat or curved surface elements, and overall. A final overall conclusion based on evaluations of singular potential integrals in several examples, is that, of the five integration methods considered, the Duffy method for singularity cancellation comes out to be the most accurate, the most rapidly converging with the increase of the orders of Gauss-Legendre integration formulas, and the fastest to execute.

REFERENCES

[1] M. Djordjević and B. M. Notaroš, "Double higher order method of moments for surface integral equation modeling of metallic and dielectric antennas and scatterers," *IEEE Trans. Antennas Propag.*, vol. 52, pp. 2118–2129, Aug. 2004.

[2] B. M. Notaroš, "Higher order frequency-domain computational electromagnetics," *IEEE Trans. Antennas Propag., Special Issue Large Multiscale Comput. Electromagn.*, vol. 56, pp. 2251–2276, Aug. 2008.

[3] D. R. Wilton, S. M. Rao, A. W. Glisson, D. H. Schaubert, O. M. Al-Bundek, and C. M. Butler, "Potential integrals for uniform and linear source distributions on polygonal and polyhedral domains," *IEEE Trans. Antennas Propag.*, vol. 32, no. 3, pp. 276–281, Mar. 1984.

[4] A. F. Peterson, *Mapped Vector Basis Functions for Electromagnetic Integral Equations*. London, U.K.: Morgan & Claypool, 2006.

[5] M. G. Duffy, "Quadrature over a pyramid or cube of integrands with a singularity at a vertex," *SIAM J. Numer. Anal.*, vol. 19, no. 6, pp. 1260–1262, 1982.

[6] R. D. Graglia, "On the numerical integration of the linear shape functions times the 3-D Green's function or its gradient on a plane triangle," *IEEE Trans. Antennas Propag.*, vol. 41, no. 10, pp. 1448–1455, Oct. 1993.

[7] M. S. Tong and W. C. Chew, "A novel approach for evaluating hypersingular and strongly singular surface integrals in electromagnetics," *IEEE Trans. Antennas Propag.*, vol. 58, no. 11, pp. 3593–3601, Nov. 2010.

[8] D. J. Taylor, "Accurate and efficient numerical integration of weakly singular integrals in Galerkin EFIE solutions," *IEEE Trans. Antennas Propag.*, vol. 51, no. 7, pp. 1630–1637, Jul. 2003.

[9] L. Rossi and P. J. Cullen, "On the fully numerical evaluation of the linear-shape function times the 3-D Green's function on a plane triangle," *IEEE Trans. Microwave Theory Tech.*, vol. 47, no. 4, pp. 398–402, Apr. 1999.

[10] M. Khayat and D. R. Wilton, "Numerical evaluation of singular and near-singular potential integrals," *IEEE Trans. Antennas Propag.*, vol. 53, no. 10, pp. 3180–3190, Oct. 2005.

[11] M. A. Khayat, D. R. Wilton, and P. W. Fink, "An improved transformation and optimized sampling scheme for the numerical evaluation of singular and near-singular potentials," *IEEE Antennas Wireless Propag. Lett.*, vol. 7, pp. 377–380, 2008.

[12] W. Ding and G. Wang, "Treatment of singular integrals on generalized curvilinear parametric quadrilaterals in higher order method of moments," *IEEE Antennas Wireless Propag. Lett.*, vol. 8, pp. 1310–1313, 2009.

[13] E. Jørgensen, J. L. Volakis, P. Meincke, and O. Breinbjerg, "Higher order hierarchical Legendre basis functions for electromagnetic modeling," *IEEE Trans. Antennas Propag.*, vol. 52, pp. 2985–2995, Nov. 2004.

[14] H. Yuan, N. Wang, and C. Liang, "Combining the higher order method of moments with geometric modeling by NURBS surfaces," *IEEE Trans. Antennas Propag.*, vol. 57, no. 11, pp. 3558–3563, Nov. 2009.

[15] R. Kieser, C. Schwab, and W. L. Wendland, "Numerical evaluation of singular and finite-part integrals on curved surfaces using symbolic manipulation," *Computing*, vol. 49, pp. 279–301, 1992.

[16] Sheng, Xin-Qing, and W. Song, *Essentials of Computational Electromagnetics*. Hoboken, NJ, USA: Wiley, 2011, vol. 757.

[17] F. Vipiana and D. R. Wilton, "Optimized numerical evaluation of singular and near-singular potential integrals involving junction basis functions," *IEEE Trans. Antennas Propag.*, vol. 59, no. 1, pp. 162–171, Jan. 2011.

[18] K. Sertel and J. L. Volakis, "Method of moments solution of volume integral equations using parametric geometry modeling," *Radio Sci.*, vol. 37, p. 10-(1-7), Jan.–Feb. 2002.

[19] E. M. Klopf, N. J. Šekeljić, M. M. Ilić, and B. M. Notaroš, "Optimal modeling parameters for higher order MoM-SIE and FEM-MoM electromagnetic simulations," *IEEE Trans. Antennas Propag.*, vol. 60, no. 6, pp. 2790–2801, Jun. 2012.

An Improved Design and Implementation of a Broadband Circularly Polarized Antenna

Chien-Hsing Lee and Yu-Han Chang

***Abstract*—This communication presents an improved design and implementation of a broadband circularly polarized antenna that features a size reduction, good axial-ratio bandwidth and good return loss bandwidth. The circuit comprises one Schiffman phase shifter that is used to obtain a wideband phase difference of 90°, and a pair of orthogonally positioned linearly polarized slot antennas with equal radiation strength that are used to accomplish a circular polarization by combining the horizontally and vertically polarized waves with a Wilkinson power divider. Measured results show that the 3 dB axial-ratio bandwidth of the proposed antenna can reach 81.5% (1.6–3.8 GHz), and the 10 dB return loss bandwidth is 100% (1.48–4.47 GHz).**

***Index Terms*—Broadband circularly polarized antenna, phase shifter, slot antenna, Wilkinson power divider.**

I. INTRODUCTION

Recently, circularly polarized (CP) antennas have been widely used in mobile communications systems. In the case of CP waves, three conditions must be satisfied, including a pair of linearly polarized (LP) waves must have equal magnitude, the two LP waves must be orthogonal to each other, and the two orthogonal LP waves are independently excited with a 90° phase shift. Although many broadband CP antennas with a 3 dB axial-ratio bandwidth of 30∼77% and a 10 dB return loss bandwidth of 35∼80% have been proposed [1]–[8] and there have been devoted to design a better and wider bandwidth CP antenna, the proposed antenna as shown in Fig. 1 was made from lower cost easily obtainable materials that it can achieve the 3 dB axial-ratio bandwidth of 81.5% and 10 dB return loss bandwidth of 100%. As seen from Fig. 1, the antenna comprises one Schiffman phase shifter (SPS) [9] and a pair of orthogonally positioned LP slot antennas. The reason to use two slot antennas is that one is to produce vertical LP radiation and the other is to provide horizontal LP radiation. The two LP modes can be realized

Manuscript received August 24, 2013; revised January 17, 2014; accepted February 20, 2014. Date of publication March 05, 2014; date of current version May 29, 2014.

The authors are with the Department of Systems and Naval Mechatronic Engineering, National Cheng Kung University, Tainan 701, Taiwan, R.O.C. (e-mail: chienlee@mail.ncku.edu.tw; y.h.jhang@hotmail.com).

Color versions of one or more of the figures in this communication are available online at http://ieeexplore.ieee.org.

Digital Object Identifier 10.1109/TAP.2014.2309962